



Trans. Nonferrous Met. Soc. China 21(2011) 2605-2609

Transactions of Nonferrous Metals Society of China

www.tnmsc.cn

# Microstructure and tensile properties of containerless near-isothermally forged TiAl alloys

HE Wei-wei<sup>1, 2</sup>, TANG Hui-ping<sup>1</sup>, LIU Hai-yan<sup>1</sup>, JIA Wen-peng<sup>1</sup>, LIU Yong<sup>2</sup>, YANG Xin<sup>1, 2</sup>

- 1. State Key Laboratory for Porous Metals Materials, Northwest Institute for Nonferrous Metal Research, Xi'an 710016, China;
  - 2. State Key Laboratory of Powder Metallurgy, Central South University, Changsha 410083, China

Received 30 July 2011; accepted 9 October 2011

**Abstract:** Ti–47Al–2Nb–2Cr–0.4(W, Mo) (mole fraction, %) alloy ingot fabricated using vacuum consumable melting was containerless near-isothermally forged, and the high temperature forgeability, microstructure and tensile properties were investigated. The results show that the TiAl ingot exhibits good heat workability during containerless near-isothermally forging process, and there are not evident cracks on the surface of as-forged TiAl pancake with a total deformation degree of 60%. The microstructure of the TiAl ingot appears to be typical nearly-lamellar(NL), comprising a great amount of lamellar colonies ( $\alpha_2$ + $\gamma$ ) and a few equiaxed  $\gamma$  grains. After near-isothermally forging, the as-forged pancake shows primarily fine equiaxed  $\gamma$  grains with an average grain size of 20 µm and some broken lamellar pieces, and some bent lamellas still exist in the hard-deformation zone. Tensile tests at room temperature show that ultimate tensile strength increases from 433 MPa to 573 MPa after forging due to grain refinement effect. **Key words:** TiAl alloy; microstructure; tensile property; containerless near-isothermal forging; grain refinement

#### 1 Introduction

Due to the attractive combination of low densities, high specific yield strength, outstanding oxidation resistance as well as good elevated temperature strengths, TiAl based alloys have been considered one of the most promising candidates for advanced structural materials for high-temperature applications in aerospace and automotive industries [1–4]. However, the low room temperature ductility and poor formability limit the extensive application of TiAl based alloys. Hot working operation is an effective way to develop a fine, uniform microstructure suitable for subsequent process or final heat treatment for desired microstructure. Therefore, considerable efforts have been devoted to studying the hot working and its effect on microstructure and mechanical properties [5–7].

Among those operations, forging is an extremely effective process and has been widely used by many investigators for manufacturing TiAl products with tailored microstructures and excellent room temperature

mechanical properties. In these researches, the forged TiAl billet was mostly canned with some metal containers [8–14]. In the present work, the containerless near-isothermally forging of TiAl alloy, including three-step deformation with short intermediate heat-treatment between the every double deformation, was carried out, and the effect of containerless forging on microstructure and tensile properties of TiAl alloys were investigated.

### 2 Experimental

The alloy with a nominal composition of Ti-47Al-2Nb-2Cr-0.4(W, Mo) (mole fraction, %) alloy ingot was prepared by vacuum arc re-melting (VAR) process three times in order to reduce composition heterogeneity. The parent materials used in this study contained high purity Ti sponge, Al, Cr, Al-Nb and Al-Mo-W-Ti interalloys. The forging billet with dimensions of *d*65 mm×90 mm was machined from the ingot, which was firstly coated with glass powder slurry to assure lubricating and to protect the billet in the

forging process, and then heated to 1200 °C in a muffle furnace for 1 h. After heating, the billet was three-step near-isothermally forged on a hydraulic presser with 6300 kN using a nominal strain rate of  $5 \times 10^{-3}$  s<sup>-1</sup>, and the die was heated and maintained at 900 °C. After the first deformation, the forged pancake was coated with glass powder slurry again, then conducted a heat-treatment at a temperature of 1200 °C for 30 min before the next step deformation. To avoid the cracking and control the grain growth, the height reduction during every step should not exceed 20% of the primal height of forging billet. The resulting pancake was crack-free and had a height of 36.2 mm, which corresponded to a deformation degree of approximately 60%.

Microstructures before and after the forging were analyzed by optical microscopy (OM). For OM observation, samples were mechanically polished and etched with Kroll's reagent (1 mL HF + 3 mL HNO<sub>3</sub> + 16 mL H<sub>2</sub>O). Phase analysis for ingot and as-forged material was conducted by X-ray diffraction (XRD) technique using Cu K<sub>a</sub> radiation. The cross-section of the oxidized pancake surface was examined on a scanning electron microscope (SEM). The microscope was equipped with an energy dispersive spectroscope (EDS) operated at 20 kV. The tensile tests of ingot and as-forged TiAl alloys were conducted at 25 °C in air on a MTS testing machine at a strain rate of  $1 \times 10^{-3}$  s<sup>-1</sup>. The specimens were prepared by electric discharge machining (EDM) in a form of plate with gauge size of 26 mm×3 mm×2 mm. The fracture surfaces of the specimens after tensile test were examined using secondary electron imaging in SEM.

### 3 Results and discussion

### 3.1 Macrostructure and exterior oxidized layer of asforged TiAl pancake

Through containerless forging with a total deformation degree of 60%, the TiAl pancake exhibits a regular shape with a thin oxidized layer, and there is no evident cracks on the surface of as-forged TiAl pancake. Figure 1 presents the macrostructure photographs of upper and cross-section of forged pancake. As seen from Figs. 1(a) and (b), the deformation structure accords to the conventional forging, which exhibits uniform single-drum and three typical deformation areas: the near surface zone of TiAl pancake is hard deformation area, the center zone of pancake is free deformation area, and the near side zone of pancake is homogeneous deformation area [15]. The metal flowing of as-forged pancake is wide and its axis is gradually perpendicular to the orientation of forging.

Figure 2 shows the SEM image and composition line scan map of the cross-section oxidized surface. As

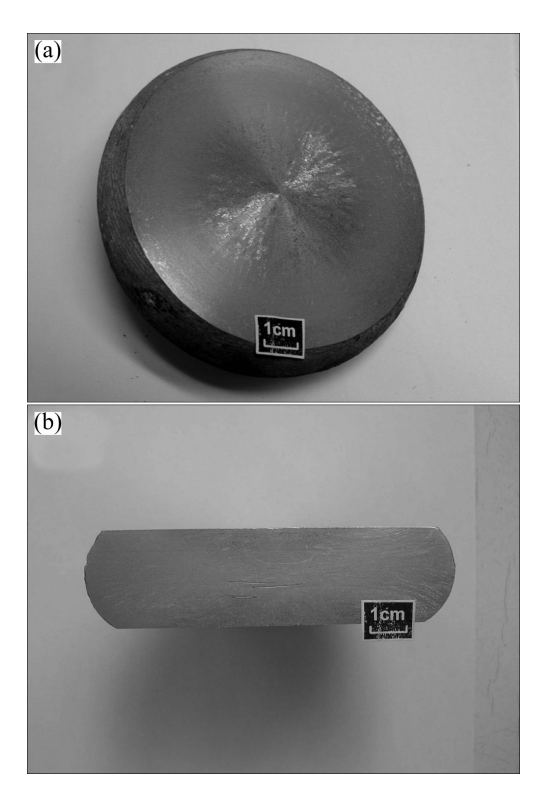
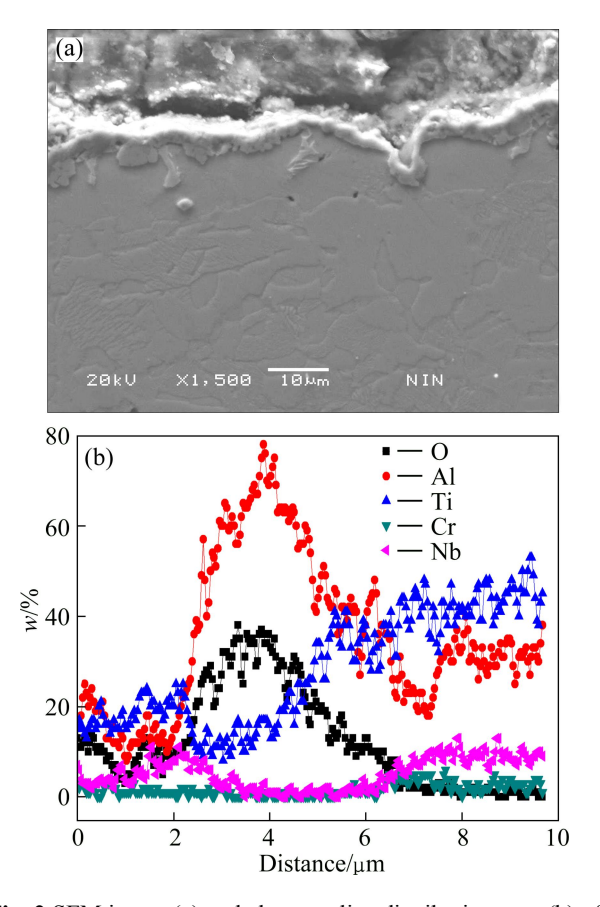


Fig. 1 Macrostructures of as-forged TiAl pancake: (a) Upper surface; (b) Cross-section



**Fig. 2** SEM image (a) and elements line distribution map (b) of cross-section of oxidized TiAl pancake surface

shown in Fig. 2, the oxide scale formed in the forging process is thin, with a thickness of 3-6 µm, and no scale spallation with cracks is observed. The elements line distribution map confirms that the oxide scale consists primarily of Al<sub>2</sub>O<sub>3</sub>, the exterior oxide scale contains more Nb element, and the aluminum-depleted layer exists at the interface of oxide scale and matrix. It is obvious that the coated glass powder slurry improves the oxidation resistance of TiAl matrix. Owing to the low level of oxidation, only Al<sub>2</sub>O<sub>3</sub> is formed in the oxide scale. This is ascribed to the fact that glass powder slurry outside the matrix acts as a barrier to the air, which can change the partial pressure of oxygen and oxidation kinetics of the matrix, leading to diffusing of aluminum towards the surface firstly and formation of denser Al<sub>2</sub>O<sub>3</sub> layer. What is more, Nb element can reduce the energy to form Al<sub>2</sub>O<sub>3</sub>, and inhibit the formation of TiO<sub>2</sub> through decreasing the concentration of O element vacancy. Thus, the oxide layer of pancake is mainly Al<sub>2</sub>O<sub>3</sub>, and the denser Al<sub>2</sub>O<sub>3</sub> layer is very useful to keep oxygen from permeating in the TiAl matrix, by which the growth of the oxide can be retarded greatly.

### 3.2 Microstructure of TiAl ingot and as-forged TiAl pancake

Figure 3 shows the microstructure of transverse section of TiAl ingot. TiAl ingot is typical nearly-lamellar microstructure, comprising a great amount of lamellar colonies  $(\alpha_2+\gamma)$  and a few equiaxed  $\gamma$ grains, and the equiaxed y grains with size of 20-50 µm exist at the interface of lamellar colonies. The grain colony size is 200-300 µm. After three-step containerless near- isothermally forging, the optical microstructure of the pancake in different deformation area is shown in Fig. 4. The microstructure of the near surface zone comprises streamlined or bent lamellar and a small amount of recrystallization duplex grain (Fig. 4(a)), while the microstructure of the center area is similar to that of the near side area, primarily comprising duplex structure with grain size of 20-30 um. It can be seen in Figs. 4(b) and (c) that, most initial lamellar

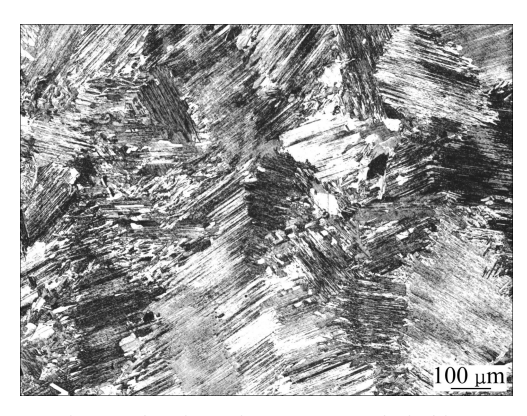
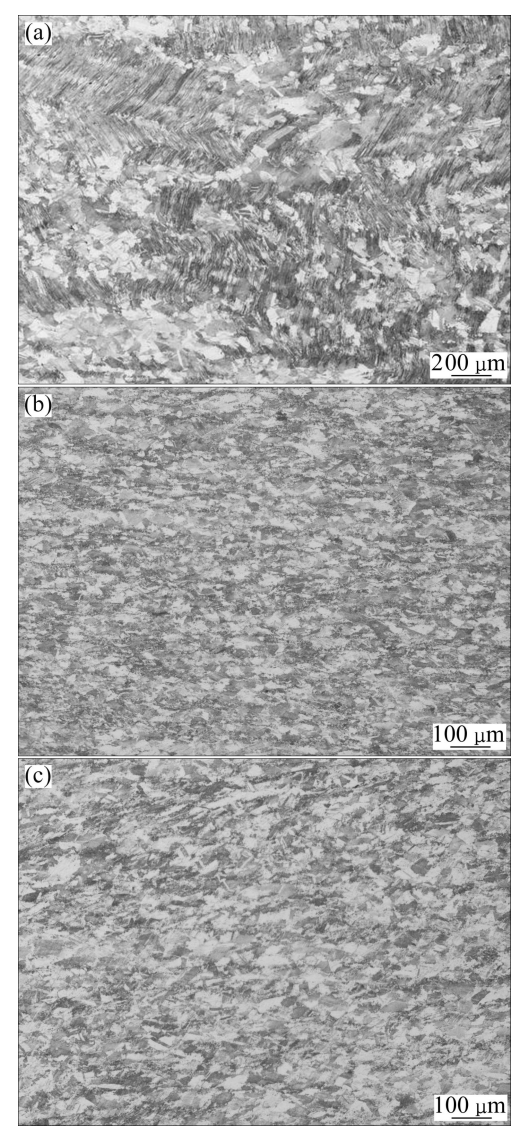


Fig. 3 OM image showing microstructure of TiAl ingot



**Fig. 4** OM images showing microstructures of as-forged pancake: (a) Near surface zone (Hard deformation area); (b) Center zone (Free deformation area); (c) Near side zone (Homogeneous deformation area)

colonies in these two areas are totally broken up, whose microstructure primarily consists of fine equiaxed  $\gamma$  grains and a litter amount broken lamellar pieces. The phase analysis of TiAl ingot and as-forged pancake (Fig. 5) confirms the presence of  $\gamma$  and  $\alpha_2$ , while peaks for remanent  $\beta$  phase are not distinct in this result. The phases of TiAl ingot and as-forged pancake do not show much difference, and they all comprise a great amount of  $\gamma$  and a few  $\alpha_2$ .

The TiAl ingot used for forging has near lamellar microstructure, showing a columnar character. Under hot-working conditions, the deformation of the lamellar colony is highly dependent on its orientation with the pressure direction and its location in the ingot. In different deformation area, the deformation behavior of the  $(\alpha_2+\gamma)$  lamellar colony is also influenced by its

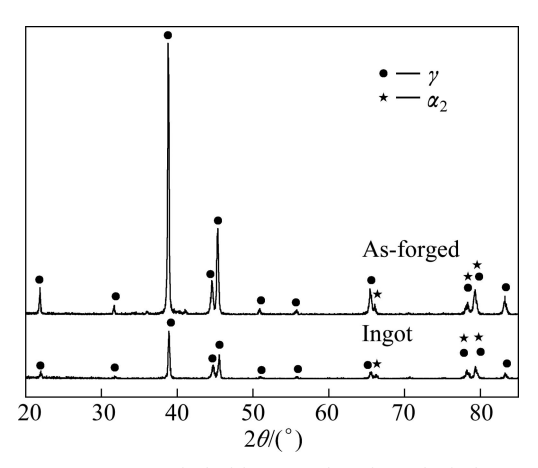
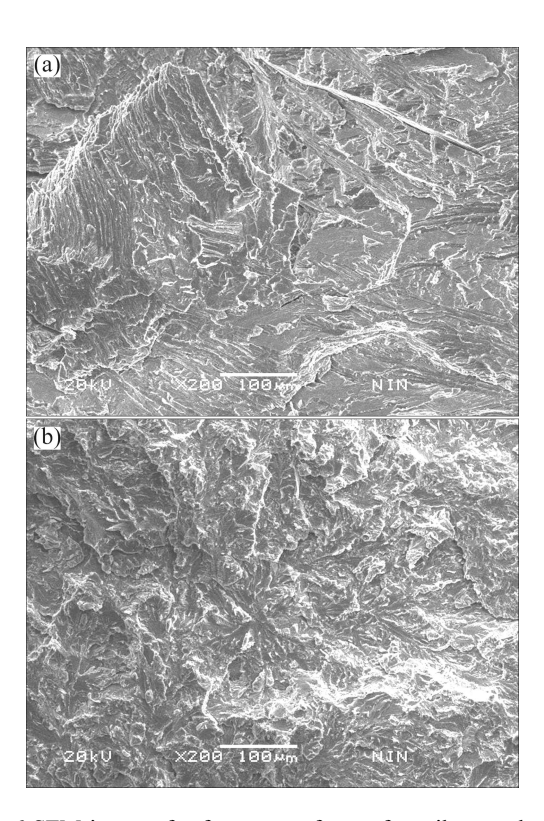


Fig. 5 XRD patterns of TiAl ingot and as-forged TiAl pancake

location in the ingot. In the near surface zone, deformation is hindered, and a great amount of lamellar colonies are not broken for the minor deformation ratio, but bend to form the wave shape structure. In the center zone, the secondary tensile stress resulting form the lateral flow of the ingot promotes the lamellar colonies to deform. During the process, the movement of the colonies leads to the shearing of the  $(\alpha_2+\gamma)$  lamellar colony boundary, which will be broken, and some end of lamellar will fracture to form small  $\alpha_2$  or  $\gamma$  particles. In the near side zone, as the deformation is homogeneous, most of the lamellar colonies will deform through bending, rotating or forming of fine-grained shearing zone in colony boundaries [12]. In addition, dynamic recrystallization (DRX) and globalization of the lamellar is also responsible for the microstructure evolution of TiAl ingot. In the area of high strain deformation, as large strain and great dislocation propagate in the lamellar boundary, a great amount of strain energy is stored in the vicinity of lamellar boundary, so that the driving force for DRX and globalization of the lamella is strong enough to promote the formation of the fine grain of DRX near the lamellar boundary. After the first deformation, a heat-treatment at 1 200 °C is conducted before the next step deformation. During heat-treatment period, the static globularization of bent lamellae with high distortion energy as well as those micro-fine grain resulting from the DRX takes place. Additionally, some lamellas are broken remarkably into fine pieces, which provide the necessary condition for DRX in the next deformation [10, 16]. In this way, TiAl pancake with microstructures mentioned above is obtained.

## 3.3 Tensile properties of TiAl ingot and as-forged TiAl pancake

The specimens of as-forged pancake for the tensile tests were exclusively excised from the easy deformation zone along tensile axis perpendicular to the forging direction. The mean ultimate tensile strength (UTS) of ingot at room temperature increases from 433 MPa to 573 MPa after containerless near-isothermally forging. Figure 6 shows the fractographs of the TiAl ingot and as-forged pancake. Transgranular fracture with numerous cleavage planes as the predominant mode is observed in the TiAl ingot, and no dimples are observed. The fracture of as-forged TiAl pancake is also dominantly transgranular cleavage-like failure, including translamellar cleavage and delamination. The TiAl ingot has inferior strength at room temperature, which is attributed to the following reasons. In general, nearly lamellar (NL) microstructure in ingot materials exhibits lower room temperature strength and higher Brittle-to-ductile transition temperature (BDT) because of the strain incompatibility and the anisotropic tensile properties [17]. The difference in properties of TiAl ingot before and after forging can be attributed to the microstructure change caused by the forging. The coarse lamellar colonies lead to lower strength. While the as-forged TiAl pancake with finer duplex (DP) microstructure shows a high tensile strength.



**Fig. 6** SEM images for fracture surfaces of tensile samples for TiAl ingot (a) and as-forged TiAl pancake (b)

### 4 Conclusions

1) The microstructure of TiAl ingot is typical nearly-lamellar, which comprises lamellar colonies and a few equiaxed  $\gamma$  grains, and the size of lamellar colonies is 200–300  $\mu$ m. In  $(\alpha+\gamma)$  phase region the TiAl alloy has

good workability.

- 2) After containerless near-isothermally forging, the as-forged alloy has fine, DP microstructure with grain size less than 20  $\mu$ m. Some bent lamellas still exist in the hard-deformation zone.
- 3) Forging can improve the tensile properties of the alloy, with an increased UTS from 433 MPa to 573 MPa at room temperature, which is the result of the grain refinement and microstructure uniformity due to large formation.

#### References

- [1] HU D, WU X, LORETTO M H. Advances in optimisation of mechanical properties in cast TiAl alloys [J]. Intermetallics, 2005, 13(9): 914–919.
- [2] WU X H. Review of alloy and process development of TiAl alloys[J]. Intermetallics, 2006, 14(10-11): 1114-1122.
- [3] DIMIDUK D M. Gamma titanium aluminide alloys-an assessment within the competition of aerospace structural materials [J]. Materials Science and Engineering A, 1999, 263(2): 281–288.
- [4] APPEL F, BROSSMANN U, CHRISTOPH U, EGGERT S, JANSCHEK P, LORENZ U, MULLAUER J, OEHRING M, PAUL D H. Recent progress in the development of gamma titanium aluminide alloys [J]. Advanced Engineering Materials, 2000, 2(11): 699-720.
- [5] CLEMENS H, KESTLER H. Processing and applications of intermetallic γ-TiAl-based alloys [J]. Advanced Engineering Materials, 2000, 2: 551–570.
- [6] SEMIATIN S L, SEETHARAMAN V, WEISS I. Hot workability of titanium and titanium aluminide alloys-an overview [J]. Materials Science and Engineering A, 1998, 243: 1–24.
- [7] GERLING R, CLMENS H, SCHIMANSKY F P. Powder metallurgical processing of intermetallic gamma titanium aluminides

- [J]. Advanced Engineering Materials, 2004, 6: 23-38.
- [8] EDWARD A L. Gamma titanium aluminides as prospective structural materials [J]. Intermetallics, 2000, 8(9–11): 1339–1345.
- [9] SUN J, HE Y H, WU J S. Characterization of low-temperature superplasticity in a thermomechanically processed TiAl based on alloy [J]. Materials Science and Engineering A, 2002, 329–331: 885–890.
- [10] KIM H Y, HONG S H. Effect of microstructure on the high-temperature deformation behavior of Ti-48Al-2W intermetallic compounds [J]. Materials Science and Engineering A, 1999, 271(1-2): 382-389.
- [11] WANG L, LIU Y, ZHANG W, WANG H, LI Q. Optimization of pack parameters for hot deformation of TiAl alloys [J]. Intermetallics, 2011, 19: 68–74.
- [12] LIU Yong, WEI Wei-feng, HUANG Bai-yun, HE Shuang-zhen, ZHOU Ke-chao, HE Yue-hui. Effect of can parameters on canned-forging process of TiAl base alloy (I)—Microstructural analyses [J]. Transactions of Nonferrous Metals Society of China, 2002. 12(4): 596–600.
- [13] LIU Yong, HE Shuang-zhen, HUANG Bai-yun, WEI Wei-feng, HE Yue-hui, ZHOU Ke-chao. Effect of can parameters on canned-forging process of TiAl base alloy (II)—Mechanical behavior [J]. Transactions of Nonferrous Metals Society of China, 2002, 12(4): 601–604.
- [14] KONG F T, CHEN Y Y, YANG F. Effect of heat treatment on microstructures and tensile properties of as-forged Ti-45Al-5Nb-0.3Y alloy [J]. Intermetallics, 2011, 19: 212–216.
- [15] LU Yan. Theory and processing of forging and pressing [M]. Beijing: China Machine Press, 1991: 128–130. (in Chinese)
- [16] XU X J, LIN J P, WANG Y L, LIN Z, CHEN G L. Deformability and microstructure transformation of pilot ingot of Ti-45Al-(8-9) Nb-(W, B, Y) alloy [J]. Materials Science and Engineering A, 2006, 416: 98-103.
- [17] KIM Y W, DIMIDUK D M. Ordered intermetallic alloys, (Part III): Gamma titanium aluminides [J]. JOM, 1994, 46(7): 30–39.

### 无包套近等温锻造 TiAI 合金的显微组织和拉伸性能

贺卫卫1,2、汤慧萍1、刘海彦1、贾文鹏1、刘 咏2、杨 鑫1,2

- 1. 西北有色金属研究院 金属多孔材料国家重点实验室, 西安 710016;
  - 2. 中南大学 粉末冶金国家重点实验室, 长沙 410083
- 摘 要: 以真空自耗电弧熔炼技术熔炼名义成分为 Ti-47AI-2Nb-2Cr-0.4(W,Mo)(摩尔百分数)的 TiAI 合金铸锭,并以该熔炼铸锭进行无包套的近等温锻造实验,研究该 TiAI 合金铸锭的高温可锻性、显微组织及拉伸性能。结果表明: 在无包套的近等温锻造工艺中,该熔炼铸锭显示出较好的高温可锻性,经涂覆玻璃粉浆保护,铸锭在经过60%锻造变形后其锻饼表面无明显裂纹。TiAI 合金的铸造组织由细小、均匀的层片状晶团( $\alpha_2+\gamma$ )和少量存在于片层团界的等轴  $\gamma$  晶粒构成;经近等温锻造后,锻饼组织则主要由平均晶粒尺寸为  $20~\mu m$  的等轴  $\gamma$  晶粒和一些破碎的片层组织构成,在一些难变形区域,依然存在弯曲变形的片层组织。室温拉伸性能检测表明,由于晶粒细化效应,锻饼的平均抗拉强度由铸锭的 433~MPa 提高到 573~MPa。

关键词: TiAl 合金; 显微组织; 拉伸性能; 近等温锻造; 晶粒细化